

Multiscale simulations of the injection moulding of a diffractive optical element

Terje Tofteberg * and Erik Andreassen
SINTEF Materials and Chemistry, Oslo, Norway
* e-mail: terje.tofteberg@sintef.no

Abstract

Simulations and injection moulding experiments for a diffractive grating are presented. The grating consists of an irregular wave pattern with wave height $0.6\ \mu\text{m}$ and wavelength $3\ \mu\text{m}$ on a $1.2\ \text{mm}$ thick part. This microfeatured part was replicated in a DVD grade polycarbonate. The degree of replication, as measured with white light interferometry and atomic force microscopy, increases with increasing mould temperature, injection velocity and holding pressure, and is high at optimal settings. 2D simulations of the filling were performed in CFX, a general Computational Fluid Dynamics code. The focus is on the coupling between the filling of the main part and the filling of the microfeatures. These filling simulations must be performed separately because of the different size scales. The rheology of the polymer is represented by a Cross – WLF model. A VOF method is used to capture the free surface and the wall has a constant heat transfer coefficient. We use as boundary condition in a local simulation around the microfeatures, the velocity field from an analytical solution of a fluid injected between two parallel plates. The reported simulations indicate that the common approach to use the pressure field at the wall as a boundary condition in the microscale simulation is neglecting important effects.

1. Introduction

This year the commercial production of CDs has been around for 25 years. Hence, microfeatured polymer discs are established as mass-produced articles for the consumer market. During this quarter of a century the development of optical storage devices has increased the storage capacity from 700 MB on the first CDs to 50 GB on the present dual layer Blu-ray Disc, partly because of the increased ability to replicate smaller features more accurately in polymeric materials. The cycle time required to make a CD has also fallen from 27 s in 1982 to 3 s today, making the products cheaper.

As is the case for conventional injection moulding, simulations can be a valuable tool to predict and explain the quality of a replicated pattern. Several authors have reported that increasing the mould temperature and the injection velocity improves the replication of microfeatures¹⁻⁴, but simulations giving quantitative predictions to these phenomena are limited. The conventional approach to model the injection phase of injection moulding is to treat the polymer as a compressible, generalized Newtonian fluid with a no-flow temperature, under which the polymer ceases to flow. The walls in the mould have a no-slip condition and a heat transfer coefficient is used to model heat transfer to the mould (typically steel).

This paper starts with a summary of some of the literature dealing with simulation of injection moulding of microfeatured parts. Then some experimental results are reported from injection moulding of a diffractive optical element (DOE) with features in the sub micrometer range. Finally, in the simulation section we give a suggestion on how to couple the different size scales in filling simulations of parts with microfeatures. In the simulations we have been using Ansys CFX 11.0, a general purpose computational fluid dynamics code based on the finite volume method.

There are two main problems linked to the simulation of parts with microfeatures. One is linked to the fact that other physical phenomena may become relevant on the microscale where wall slip⁵, surface tension⁶ and microrheology⁷ can have important influence on the flow. The other is linked to the multiscale nature of the problem and this is what we will focus on in this work; how to couple large scale flow with microscale flow. The conventional approach with a generalized Newtonian fluid will still be used.

In our case we are injection moulding a diffractive grating with structural details down to 100 nm. These features are located on the surface of a part with thickness 1.2 mm or 10.000 times larger than the microfeatures. To perform a 3D simulation where both the submicron details and the overall geometry of the part are included does not seem possible with today's methods. The mesh size and time step required for sufficient resolution in the microfeatures would create a number of mesh elements and a number of time steps too large to handle in the main geometry.

1.1 Previous simulations on microfeathered components

The first strategy to reduce the number of mesh elements is to use an element size that is getting smaller when approaching the microstructure. Yu et al⁸ tried this method when simulating the filling of a plate with a microstructure. The microstructure was a rib with thickness 0.2 mm, height 0.5 mm and length 2 mm. The thickness of this rib was only one tenth of the thickness of the part, but we still include it here as a microfeathered component because it illustrates a common problem found when simulating phenomena on different size scales. They tried both a Hele-Shaw and a full 3D simulation with a mesh that was successively getting finer when approaching the microstructure. In the Hele-Shaw case the flow front was unphysically slowed down when approaching the microstructure. This was not observed in the 3D-case. Generally it is not recommended to have large size gradients in the mesh when simulating free surface flows. It is also necessary to reduce the time step in the simulation significantly so that the flow front does not pass through too many elements in the microstructure for each time step.

The second strategy is to reduce the computational domain by performing two coupled simulations on different size scales. The most basic way to do this coupling in injection moulding is to run a conventional simulation of the main geometry without the microfeatures. From this simulation the distribution of pressure and temperature and the volume occupied by polymer as a function of time, are extracted. Then a new simulation is made where only the microstructure is included and the data from the main geometry simulation is used as a boundary condition.

This approach was used by Yao and Kim⁶ who performed injection moulding and simulation of a plate with 40 μm thick ribs (aspect ratio 10) in HDPE. In their simulations they performed first a large scale simulation considering the filling of the plate and then a local simulation of the isolated microstructure. Both experimentally and in simulations they found that the ribs were only filled when the temperature of the mould exceeded the melting temperature of the polymer.

The same kind of coupling was also used by Kim and Turng⁹. They extracted the temperature and the pressure from a large scale simulation and coupled these to a small scale simulation. They found that the simulated results were strongly dependent on the heat transfer coefficient chosen. At higher injection velocities they found it necessary to use a higher heat transfer coefficient in order for the simulations to agree with experiments.

Eriksson and Rasmussen¹⁰ performed isothermal simulations and compression moulding experiments of 10 μm deep channels (aspect ratio 0.5) in PC and PS. In their 2D simulations they used a linear viscoelastic model for the melt. They first performed a macroscale

simulation of the injection of polymer melt between two plates in a Lagrangian frame of reference. In the subsequent microscale simulation, they used the normal and tangential stresses at the wall in the first simulation as a boundary condition. In addition, since they used a viscoelastic model, also the deformation history at the wall was provided at the start of the microscale simulation. This is a more sophisticated method than the ones previously described, but it still uses the pressure at the wall in the large scale simulation as a boundary condition in the microscale simulation. However, they do not set this as a boundary condition directly at the microfeature but include parts of the bulk flow in their local simulations.

2. Experimental

2.1 Nickel shim (mould insert) and injection moulding of diffractive optical elements

We have studied the injection moulding of a diffractive optical element (DOE) and when we in the rest of the article refer to the DOE, this will mean the injection moulded part, and, in particular, the microfeatured area on this part. The microfeatured area consists of an irregular wave pattern designed by Løvhaugen et al¹¹, which covers an area of 1 cm x 1 cm. A section of this design can be seen in **Figure 1**. The main pattern is an irregular wave with a typical wave height of 600 nm and a wavelength of 3 μm . Orthogonal to this there is a secondary wave pattern with wavelength $< 1 \mu\text{m}$. The Ni shim is made by first using e-beam lithography to pattern a photoresist with a topographical pattern. The photoresist is electroplated with Ni to give a Ni shim and a further Ni replica is made of this one to be used as a mould insert for the injection moulding of DOEs.

The injection moulding is performed on a Battenfeld EM 50/120 machine with a DVD grade polycarbonate (*GE plastics, Lexan OQ 1026*), with a glass transition temperature of 145 - 150°C. The parts, shown schematically in **Figure 2**, were produced with different settings for the mould temperature (60 - 120 °C), the flow front velocity (130 - 1300 mm/s) and the holding pressure (10 – 100 MPa), as measured ahead of the machine nozzle.

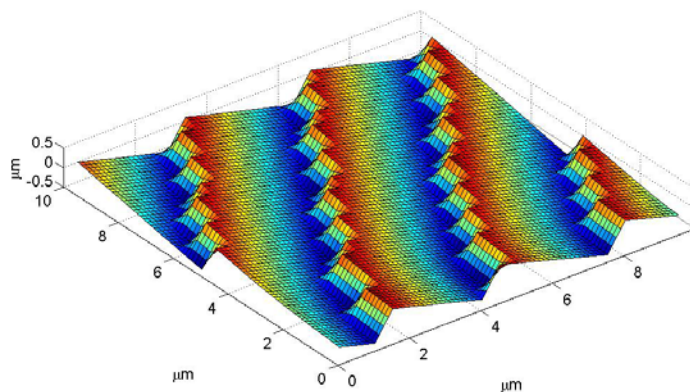


Figure 1 A section of the DOE topography. The design consists of five superimposed wave patterns and is thus irregular. The main features are similar to the section shown, covering a total area of 1 cm x 1cm.

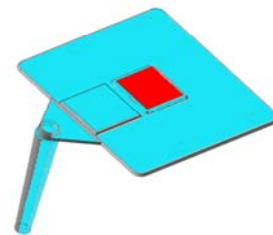


Figure 2 The geometry of the injection moulded part. The microfeatured area (the DOE) is shown in red, and has a topography as shown in Figure 1.

2.2 Characterisation

Topographical images of the produced DOEs and the Ni shim were recorded using a white light interferometer (WLI), WYKO NT-2000. The maximum resolution possible is 0.5 μm in the plane and 10 nm vertically. To measure the replication quality, 45 μm x 60 μm images near the center of the 1 cm x 1 cm microstructured area were recorded of the Ni shim and the DOEs. Even though the pattern was irregular and the WLI images were not always recorded at the exact same location, we wanted a scalar measure of the degree of replication. The method chosen is sketched in **Figure 3** and described in the following.

First the autocorrelation function (ACF) of the topographical image $h(x,y)$ was found.

$$ACF(x, y) = \int_0^{L_x} \int_0^{L_y} h(x - \tilde{x}, y - \tilde{y}) h(x, y) d\tilde{x} d\tilde{y} \quad (1)$$

Here the integration is over the whole image recorded and a periodic boundary is assumed. Secondly, the Power Spectrum Density (PSD) was calculated by taking the Fourier transform of this signal orthogonal to the wave pattern and averaged in the x -direction.

$$PSD(f_y) = \int_0^{L_x} \frac{1}{L_x} \int_{-\infty}^{\infty} ACF(x, y) e^{i2\pi f_y y} dy dx \quad (2)$$

The largest peak in this spectrum was then located around a wavelength of 3 μm . The square root of the area under this peak has the unit length and is a measure of the average peak height. The value found for a DOE divided by the value for the Ni shim was taken as the degree of replication. It was seen that this measure corresponded well with a manual inspection of the peak height of the DOEs relative to the Ni shim. To measure the warpage, low-resolution WLI images were recorded. Some DOEs were also investigated using AFM to give high-resolution topographical images.

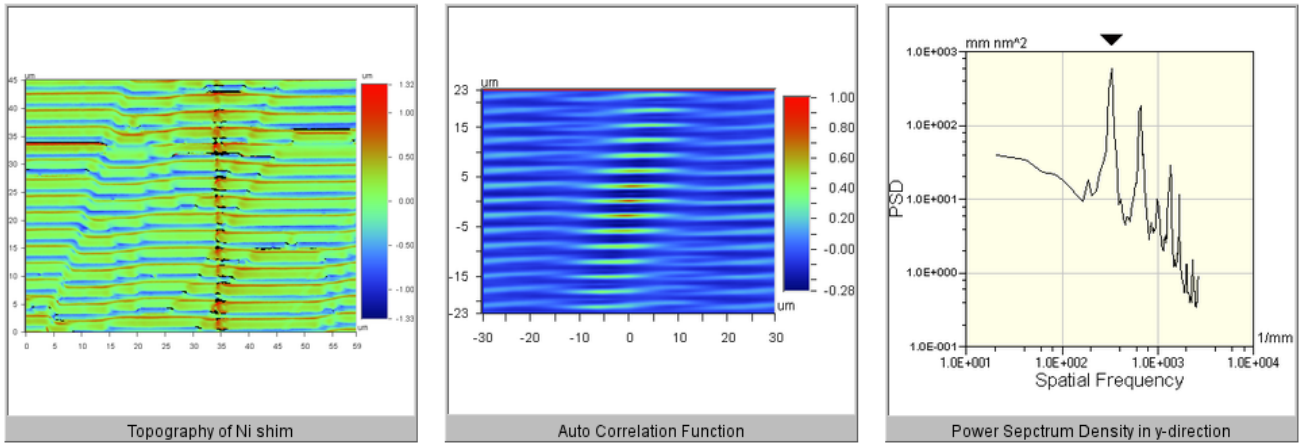


Figure 3 Sketch on how we define degree of replication, illustrated by using the Ni shim. A measure of the amplitude of the wave pattern is found by taking the Fourier transform (right) of the autocorrelation function (middle, here scaled to unity) of the topographical data (left).

3. Experimental results

3.1 White light interferometry (WLI)

The topography of the injection moulded DOEs were characterised with WLI. The degree of replication was calculated by the method sketched in **Figure 3** and is shown in **Figure 4**. We see that, as expected, the degree of replication increases with increasing injection velocity and mould temperature. It is also increased by increasing the holding pressure. At the highest setting for injection velocity, holding pressure and mould temperature, the wave height of the diffractive pattern in the polycarbonate actually seems to be higher than what was found on the Ni shim at room temperature. This was observed with both WLI and AFM by visual inspection of the wave height and was not introduced by using power spectrum density to measure replication. The reason is unknown, but it seems to be a repeatable observation.

We found that by applying a holding pressure of 39 MPa, the curvature over the microstructured area was reduced from 10 to 5 μm over 1 cm. No further improvement was seen on further increasing the holding pressure. This was within the specification tolerance of 10 μm set for the application of the DOE.

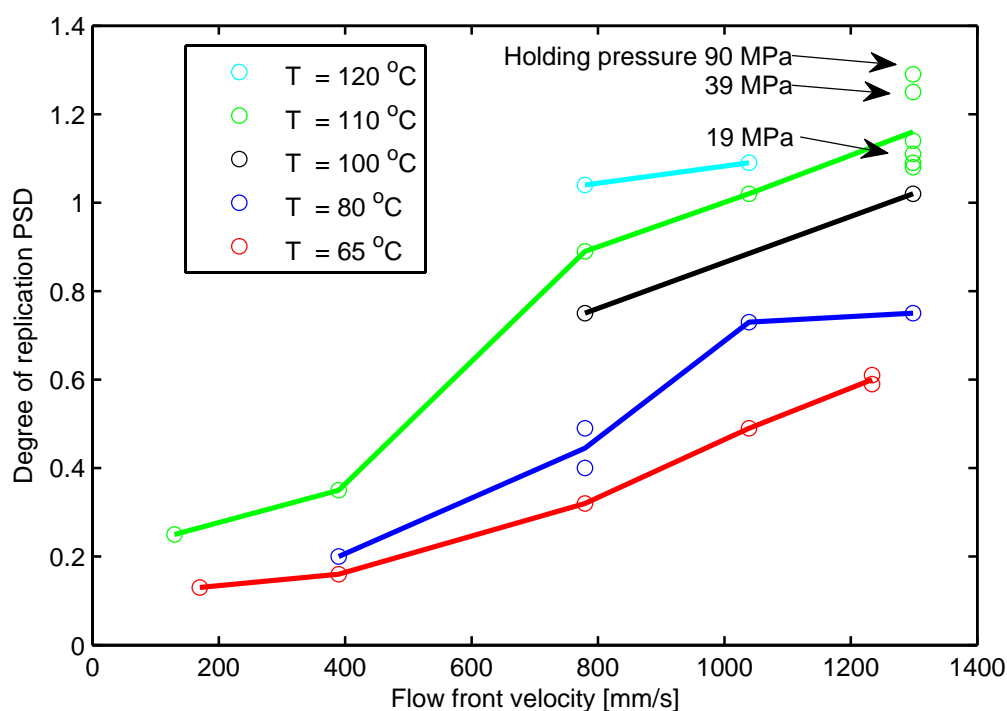


Figure 4 Degree of replication of the diffractive grating at different process settings. The procedure to determine the degree of replication is illustrated in **Figure 3**. Where nothing else is indicated, a holding pressure of 19 MPa was used.

3.2 Atomic force microscopy (AFM)

AFM images of the Ni shim and a DOE are shown in **Figure 5**. It can be seen that the microfeatures are qualitatively well replicated. Note that for perfect replication the images should be the inverted versions of each other. The Ni shim probably has some dust on it which is the reason for the small wart like structures.

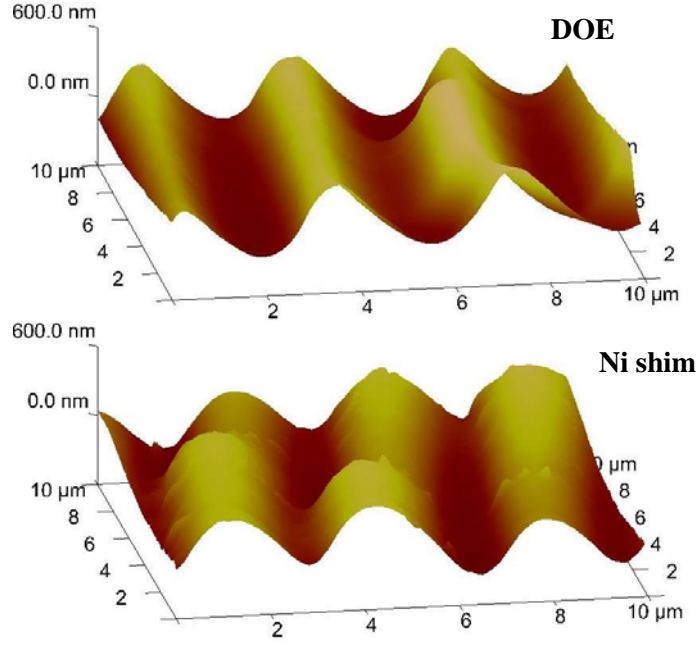


Figure 5 AFM pictures of the Ni shim and a DOE produced at the optimal setting found. The pictures are not taken from the exact same location and can thus not be directly compared, but the patterns are qualitatively similar.

4. Simulations

4.1 Governing Equations

The polymer melt and the air are treated as incompressible, and the equation of continuity is written as

$$\nabla \cdot \mathbf{u} = 0, \quad (3)$$

where \mathbf{u} is the velocity vector and ∇ the divergence operator. The fluid is treated as a generalized Newtonian fluid and the momentum balance is written

$$\rho \left(\frac{\partial \mathbf{u}}{\partial t} + \mathbf{u} \cdot (\nabla \mathbf{u}) \right) = -\nabla p + \nabla \cdot \eta (\nabla \mathbf{u} + (\nabla \mathbf{u})^T), \quad (4)$$

where t is the time, ρ the density, p the pressure and η the viscosity of the fluid. In the energy equation we include conductive and convective heat transfer.

$$\rho c_p \left(\frac{\partial T}{\partial t} + \mathbf{u} \cdot (\nabla T) \right) = \nabla \cdot (\kappa \nabla T) \quad (5)$$

T is the temperature, c_p is the heat capacity and κ is the heat transfer coefficient. In the simulations there are two different phases, the polymer melt and air. This multiphase problem is solved using a Volume of Fluid (VOF) method, first described by Hirt and Nichols¹². It involves a scalar variable, the volume fraction α , which is transported through the computational domain by convection.

$$\frac{\partial \alpha}{\partial t} + \mathbf{u} \cdot (\nabla \alpha) = 0 \quad (6)$$

In this case, when α is 0, a volume is filled with air and when α is 1, it is filled with polymer and the fluid has the properties of the pure phases. In a thin interface region, usually 2-3 mesh elements thick, the volume fraction is between 0 and 1 and the physical properties such as density and heat conductivity are taken as a linear interpolation over the volume fraction. The viscosity of the polymer is described using a five parameter Cross-WLF model.

$$\eta(T, \dot{\gamma}) = \frac{\eta_o(T)}{1 + \left(\frac{\eta_o(T) \dot{\gamma}}{\tau^*} \right)^{1-n}} \quad (7)$$

$$\eta_o(T) = \eta_r(T_r) \exp \left\{ \frac{-A_1(T - T_r)}{A_2 + T - T_r} \right\}$$

The material data for the polycarbonate is taken from the Moldflow database and are given in table 1.

Table 1 Material parameters for the polycarbonate material.

N	0.17
τ^*	849252 Pa
$\eta_r(T_r)$	1.69664E11 Pa s
T_r	417.15 K
A_1	28.704
A_2	51.6 K
P	1049.3 kg/m ³
K	0.163 W/mK
C_p	1800 J/kg K

4.2 Coupling between macro and microscale flow

A first attempt was made to simulate the filling of the DOE in Moldflow MPI using a 3D simulation with a mesh that gradually was refined when approaching the microstructure. This led to similar unphysical flow phenomena as those observed by Yu et al⁸, where the microfeatured area acts as an obstacle to flow. Because of this, a new method to couple the large scale and microscale simulations was developed.

The 2D computational domain consists of the microstructure and a surrounding area as seen in **Figure 6** where also the initial value of the volume fraction is shown. The flow front is at this time a semi-circle, which is tangential to the wall just at the start of the microstructure. At this initial time, the microfeature has not had any influence on the flow field. It can be seen that we have reduced the geometrical complexity of the diffractive grating to a triangle. This has a height 600 nm and length 3000 nm. The idea is to choose a surrounding area so large that the flow field at the boundary will not be influenced by the filling of the microstructure. We have chosen to include 0.5 % of the thickness of the plate and a downstream length long enough to keep the right edge in **Figure 6** dry during the whole simulation. We thus get information on how the microstructure is filled as the flow front passes it. In the simulation we prescribe the flow field at the bottom and left edge. On the right side there is a zero pressure outlet. Such an outlet is also included on the top of the microstructure to allow air to escape.

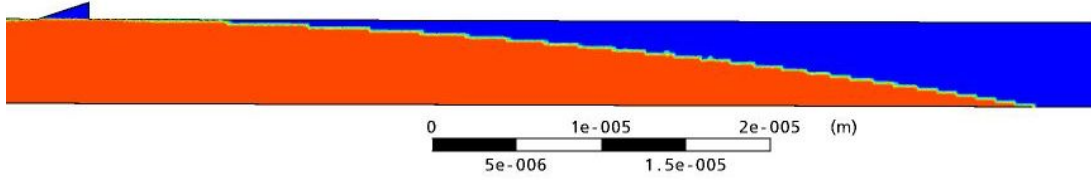


Figure 6 Initial condition for the local simulation around the microfeature (the triangle at the upper left). The area coloured red is filled with polymer. The initial temperature is uniform and the initial velocity field is taken from an analytical solution of a melt injected between two parallel plates.

The idea is to take the flow field on the left and bottom edge and the initial conditions from a large scale simulation of the whole part. So far, however, we have used an analytical solution of the flow field behind the flow front for a Newtonian fluid injected between two parallel plates. This solution was derived by Gramberg et al¹³ and they assumed that the flow front is a semicircle, an assumption that Gramberg et al describes as acceptable. Mavridis et al¹⁴ showed in numerical simulations that there are no qualitative differences between the flow field for a shear thinning fluid and that of a Newtonian fluid close to the flow front. Therefore, as a first approach, the analytical solution of Gramberg et al was used as an approximation to the flow field. The advantage using such a solution instead of a numerical solution is that we have infinite resolution close to the wall in the area of interest.

For the temperature we used the temperature at the nozzle for both initial conditions and at the left and bottom edges. This assumption is made based on an analytical solution of the temperature distribution made by Gramberg and Ven¹⁵, where they showed that only a thin layer close to the wall is cooled during injection. The material at the flow front is being transported outwards from the middle of the plate in the fountain flow and has thus not had much time to cool down before hitting the wall. This assumption is not a good one and it should be modified in further work but the simulations still give some interesting results.

At the wall we prescribe a temperature T_{wall} , a constant heat transfer coefficient h and a no slip condition.

$$\begin{aligned} \mathbf{u}_{wall} &= 0 \\ \kappa \nabla T &= h(T - T_{wall}) \mathbf{n}, \end{aligned} \quad (8)$$

where \mathbf{n} is the normal vector to the wall.

4.3 Some comments on the implementation in CFX

There are two main difficulties involved when using CFX as a simulation code. The first is the fact that fluid is present everywhere, which means that many resources are spent calculating the velocity field in regions filled with air which does not have a large influence on the flow of polymer. It is also necessary to allow air to escape by introducing venting channels.

In injection moulding simulations it is common to neglect the acceleration terms in Eq. (4) which involves setting the left hand side equal to zero due to the low Reynolds number. This simplification has not been made in the current simulations because of implementation difficulties.

These two factors increase the computational resources required to solve the injection moulding problem and thus also the simulation time. However, introducing them does not neglect any effects and if the solver performs well it should not influence the results.

CFX is a 3D finite volume solver. In order to perform a 2D simulation, a mesh is made which is only one element thick and symmetry conditions are applied at the two surfaces parallel to the computational plane.

5. Simulation results

The simulation results must be considered preliminary and do overpredict the filling of the microstructures, partly because of the unphysical thermal initial and boundary conditions. We do, however, present some interesting findings. The results presented here were found using a melt temperature of 300 °C, a flow front velocity of 300 mm/s, a mould temperature of 110°C and a heat transfer coefficient of 100 000 W/(m² K).

If we look at the pressure around the inlet to the microstructure when the flow front has just passed, as seen in **Figure 7**, we see that the pressure at the wall is significantly higher than the pressure at the inlet to the microfeature. There is a significant pressure drop linked to the transport of material from the bulk flow to the microfeature. The previously reported coupled simulations in the literature used the pressure at the wall as a boundary condition to a separate simulation of the microfeatures. The pressure drop in the bulk flow is then not accounted for even though it can be seen in **Figure 7** that it is an important factor and this assumption may lead to an overprediction of filling. It can also be noted that there is a relatively high pressure, 5 MPa just behind the flow front. In the analytical solution of Gramberg et al¹³ the pressure goes to infinity at the point where the melt, air and wall coincide. This is a result of the no-slip condition and it is assumed that the high pressure we see here is also a product of this boundary condition. In **Figure 7** the triple point is approximately 2 μm to the right of the right edge.

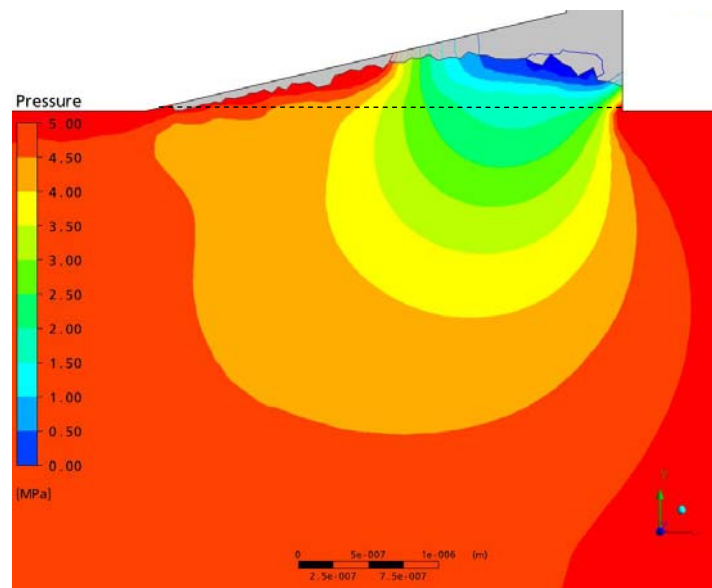


Figure 7 Pressure distribution around the inlet to the microstructure. The flow is going from left to right and the flow front has just passed the microfeature. Notice that the pressure along the dashed horizontal line is much smaller than that at the wall. The uppermost horizontal line in the figure is a pressure outlet to allow for air to escape.

For the temperature, a similar effect is shown as seen in **Figure 8**. Around the microfeature, the polymer is in contact with the wall and is therefore cooled down. On the other hand, in the microfeature, there is an insulating air gap between the polymer and the wall which make the temperature at the inlet to the microfeature higher than the temperature at the wall. This is

also an effect that it not accounted for when taking the wall temperature as a boundary condition to a separate simulation of only the microstructure.

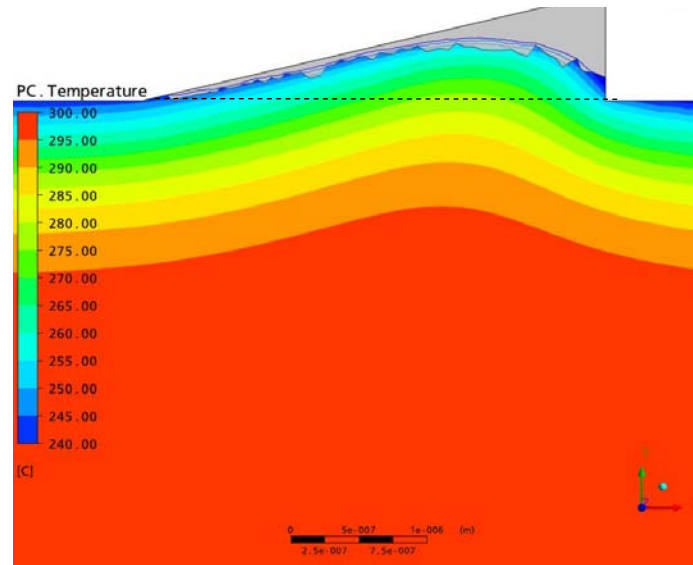


Figure 8 Temperature field around the microfeature. The flow is going from left to right and the flow front has passed the microfeature.

6. Conclusion

Our experimental work shows that our diffractive optical element can be injection moulded with a high degree of accuracy using optimal processing parameters. In accordance with previous work these settings are high mould temperature and high injection velocity in order to allow the polymer melt to fill the microfeatures before it solidifies.

Our simulations show that it is necessary to include a larger part of the geometry in a microscale simulation than only the isolated microfeature, a strategy which has been used in previous simulations in the literature. This is because the microfeature influences the temperature, pressure and flow fields of the bulk flow around it.

In order for the simulations to give physically valid results the temperature field should be coupled with macroscale simulations and further investigations should be made as to whether microscale flow effects influence the flow field.

References

- (1) Ong, N. S.; Zhang, H. L.; Woo, W. H. *Materials and Manufacturing Processes* **2006**, *21*, 824.
- (2) Su, Y.-C.; Shah, J.; Lin, L. *Journal of Micromechanics and Microengineering* **2004**, *14*, 415.
- (3) Xu, G.; Yu, L.; Lee, L. J.; Koelling, K. W. *Polymer Engineering and Science* **2005**, *45*, 866.
- (4) Zhao, J.; Mayes, R. H.; Chen, G.; Chan, P. S.; Xiong, Z. J. *Plastics, Rubber and Composites* **2003**, *32*, 240.
- (5) Chien, R. D.; Jong, W. R.; Chen, S. C. *Journal of Micromechanics and Microengineering* **2005**, *15*, 1389.
- (6) Yao, D.; Kim, B. *Journal of Injection Molding technology* **2002**, *6*, 11.
- (7) Dhinojwala, A. *Materials Science and Technology* **2003**, *19*, 1170.
- (8) Yu, L.; Lee, L. J.; Koelling, K. W. *Polymer Engineering and Science* **2004**, *44*, 1866.
- (9) Kim, S. W.; Turng, L. S. *Polymer Engineering and Science* **2006**, *46*, 1263.
- (10) Eriksson, T.; Rasmussen, H. K. *Journal of Non-Newtonian Fluid Mechanics* **2005**, *127*, 191.
- (11) Løvhaugen, O.; Johansen, I.-R.; Bakke, K. A. H.; Fismen, B. G.; Nicolas, B. G. *Journal of modern optics* **2004**, *51*, 2203.
- (12) Hirt, C. W.; Nichols, B. D. *Journal of computational physics* **1981**, *39*, 201.
- (13) Gramberg, H. J.; van Vroonhoven, J. C. W.; van de Ven, A. A. F. *European Journal of Mechanics B-Fluids* **2004**, *23*, 571.
- (14) Mavridis, H.; Hrymak, A. N.; Vlachopoulos, J. *Polymer Engineering & Science* **1986**, *26*, 449.
- (15) Gramberg, H. J. J.; van de Ven, A. A. F. *European Journal of Mechanics B-Fluids* **2005**, *24*, 767.